Structural and Functional Reconstitution of Inner Dynein Arms in *Chlamydomonas* Flagellar Axonemes

Elizabeth F. Smith and Winfield S. Sale

Department of Anatomy and Cell Biology, Emory University, Atlanta, Georgia 30322

Abstract. The inner row of dynein arms contains three dynein subforms. Each is distinct in composition and location in flagellar axonemes. To begin investigating the specificity of inner dynein arm assembly, we assessed the capability of isolated inner arm dynein subforms to rebind to their appropriate positions on axonemal doublet microtubules by recombining them with either mutant or extracted axonemes missing some or all dyneins. Densitometry of Coomassie blue–stained polyacrylamide gels revealed that for each inner dynein arm subform, binding to axonemes was saturable and stoichiometric. Using structural markers of position and polarity, electron microscopy confirmed that subforms bound to the correct inner arm position. Inner arms did not bind to outer arm or inappropriate inner arm positions despite the availability of sites. These and previous observations implicate specialized tubulin isoforms or nontubulin proteins in designation of specific inner dynein arm binding sites. Further, microtubule sliding velocities were restored to dynein-depleted axonemes upon rebinding of the missing inner arm subtypes as evaluated by an ATP-induced microtubule sliding disintegration assay. Therefore, not only were the inner arm dynein subforms able to identify and bind to the correct location on doublet microtubules but they bound in a functionally active conformation.

We previously identified three subforms of inner dynein arms which we named I1, I2, and I3 based on their location in the axoneme (Piperno et al., 1990). Biochemical and structural analyses of mutant and wild-type flagellar axonemes from *Chlamydomonas reinhardtii* revealed that I1, I2, and I3 are present in triplet groups that repeat every 96 nm along the length of the axoneme (Fig. 1). I1 is a heterodimer composed of heavy chains 1α and 1β, and is located just proximal to spoke 1. I2 and I3 are homodimers in heavy chain composition; I2 is located between spoke 1 and spoke 2, and I3 is located just distal to spoke 3. Although the composition of I1 remains the same along the entire length of the axoneme, the composition of I2 and I3 changes in proximal and distal regions (Piperno and Ramanis, 1991). Additional complexity of this arrangement is also revealed by a variety of structural approaches (e.g., Goodenough and Heuser, 1985, 1989) including recent evidence for a staggered or multi-row arrangement of inner dynein arm components (Kamiya et al., 1991; Muto et al., 1991).

Several questions about this assortment of dynein ATPases remain to be answered. First, what is the precise molecular structure of each inner dynein arm? Answers will continue to require high resolution structural and immunochemical analysis. Second, what is the function of each dynein subform? Analysis of the properties of isolated proteins by a variety of functional assays (c.f. Kagami et al., 1990; Smith and Sale, 1991) and motion analysis of mutant flagella (Brokaw and Kamiya, 1987) have begun to reveal functional properties. And, third, what is the mechanism by which I1, I2, and I3 recognize and bind to the appropriate location on A-microtubules during flagellar morphogenesis? This final question is the primary topic of this paper.

There are several models which might describe how the dynein arms assemble at correct sites along each doublet microtubule. First, perhaps once the initial inner arm binds to the first available site on the microtubule, the correct adjacent inner arm will follow in sequence along the length of the axoneme as assembly proceeds. However, this model can explain neither the correct binding of inner arms on the surface of the A-microtubule, nor the precise assembly of remaining inner arm subtypes in flagella of mutant cells missing subsets of inner arm dyneins. (c.f. Piperno et al., 1990). Thus, the correct assembly of a particular inner arm subform is not dependent on the assembly of the other subforms. Additional structural evidence supports this hypothesis. As opposed to the outer row of arms which appear to overlap each other (Goodenough and Heuser, 1982) and bind to microtubules in a cooperative manner (Haimo et al., 1979), deep-etch rotary-shadowed replicas of axonemes suggest the inner arms do not overlap (Goodenough and Heuser, 1989) and do not appear to bind microtubules in a cooperative fashion (Smith and Sale, 1991).

Another possibility is that the inner dynein arm positions are designated by spokes since these structures are in close

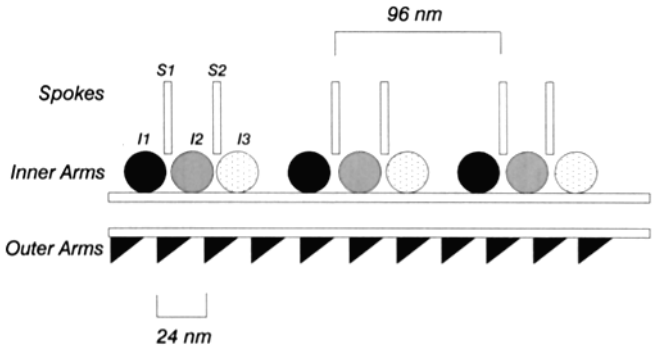

Figure 1. Model of a longitudinal view through a wild-type *Chlamydomonas* axoneme showing inner dynein arm arrangement based on data from Piperno et al. (1990). S1 and S2 represent the spokes where spoke 1 is proximal. I1, I2, and I3 represent the inner arms. I1, I2, and I3 repeat in triplet groups along the length of the axoneme in specific orientations relative to the spokes.

proximity and repeat at 96 nm in register with the inner arms. This hypothesis predicts that spokeless mutants would be defective in inner arm assembly. However, *pf*14, a spokeless mutant, retains complete rows of inner dynein arms (Muto et al., 1991), and the double mutant *pf*14*pf*30, which is missing both spokes and inner arm I1, contains the same regularly repeating gap in inner arm structure as in *pf*30 (Smith, E. F., unpublished observations). Therefore, the spokes probably do not determine the correct location of the inner dynein arms.

A third possibility is that the inner arms recognize certain specific lattice repeat patterns inherent to the doublet microtubule wall. However, structural studies have not identified obvious patterns which repeat at the predicted intervals. Rather, specialized tubulin isoforms or nontubulin adaptor proteins are most likely necessary for correct positioning of each inner arm subform.

To begin investigating this final possibility, we used an in vitro approach to test whether isolated inner arm dynein subforms would specifically rebind to correct positions on assembled mutant or extracted axonemes missing inner dynein arms. Biochemical analysis revealed that the dynein binding was saturable at the predicted stoichiometry, and EM confirmed that inner arm subforms bound to their proper location. Additionally, sliding disintegration assays revealed that microtubule sliding velocities could be recovered upon restoration of the missing inner arm dynein subforms. These results indicate that correct positioning of the inner arms is not dependent on concurrent assembly of axonemes, that nontubulin receptor proteins or tubulin isoforms, correctly positioned on the axoneme, must dictate the site of assembly of each inner dynein arm subform, and that inner arm subforms rebind in a functionally competent form.

Materials and Methods

Cell Strains and Growth Conditions

Chlamydomonas reinhardtii strains used include the outer armless mutant *pf*28 (Mitchell and Rosenbaum, 1985; Kamiya and Okamoto, 1985) and *pf*30*pf*28 which is missing both the outer dynein arms and inner arm subform I1, and is paralyzed (Piperno et al., 1990). Our original stocks of *pf*30*pf*28 contained cells that were heterogeneous in flagellar length but most of which were short. After subcloning these cultures we obtained a population of *pf*30*pf*28 cells that were homogeneous for long flagella. Biochemical and structural analyses of these paralyzed flagella indicated that they are identical in inner arm composition and organization to the *pf*30*pf*28 flagella used by Piperno et al. (1990). Cells with long flagella not only facilitated structural and biochemical studies but were an absolute requirement for the sliding disintegration assay described below. For all experiments cells were grown in liquid culture with aeration over a 14 h/10 h light/dark cycle (Witman, 1986).

Isolation of Flagella, Axonemes, and Inner Arm Dyneins

Flagella were severed from cell bodies by the dibucaine method (Witman, 1986; King et al., 1986) and isolated by differential centrifugation in Buffer A (10 mM Hepes, 5 mM $MgSO_4$, 1 mM DTT, 0.5 mM EDTA, 30 mM NaCl, 0.1 mM PMSF, and 0.6 TIU aprotinin, pH 7.4). Axonemes were isolated as described earlier (Witman et al., 1978) using 0.5% (wt/vol) NP-40 to remove flagellar membranes. To obtain crude inner dynein arm extracts, axonemes were resuspended to a concentration of 10 mg/ml in buffer A containing high salt (600 mM NaCl) and extracted for 1 h on ice. Axonemes were pelleted and the resulting supernatant was dialyzed into 30 mM NaCl Buffer A. The pelleted axonemes were resuspended in an equivalent volume of Buffer A or, in some cases, extracted once again to further remove small numbers of residual dyneins.

For obtaining isolated inner dynein arm fractions, the high salt extract was loaded onto a 5–20% sucrose gradient made with Buffer A and run for 16 h at 35,000 rpm in a rotor (model SW41; Beckman Instruments Inc., Palo Alto, CA). 20 equal fractions were collected and protein peaks were rapidly determined by gel electrophoresis on minigels composed of a 7% polyacrylamide resolving gel and a 3% stacking gel (Laemmli, 1970). The 21S peak contained I1 whereas the 11S peak contained a mixture of I2 and I3 (Piperno et al., 1990; Smith and Sale, 1991).

Reconstitution Experiments/Quantitative Analysis

Extracts and axonemes were recombined in various ratios based on volume and the original stoichiometry as described in Results. The amount of axonemes was constant for all recombinations with the amount of extract added varying. The appropriate volume of Buffer A was then added so that all final volumes were equal with a final protein concentration of 7–8 mg/ml. The mixtures were incubated at room temperature for 15 min after which the axonemes were pelleted at 15,000 rpm for 20 min in a rotor (model SS34; Sorvall Instruments Div., DuPont Co., Wilmington, DE.). Supernatants were collected, axonemes were resuspended in the appropriate volume, and samples were fixed for gel electrophoresis or electron microscopy as required.

Supernatants and pellets were run on a single polyacrylamide gel composed of a 2.5–5.0% acrylamide resolving gel with both a urea (0–8 M) and sucrose gradient (Sale et al., 1985). Inner arm heavy chain bands were identified using axonemes derived from the appropriate mutant cells as electrophoretic standards as described (Smith and Sale, 1991). Densitometry of heavy chain bands was performed by using the Image-1 System gel scanning function to measure band intensity (Universal Imaging Corporation, West Chester, PA). The values presented in accompanying figures are the result of three subtractions. First, the program automatically subtracts the baseline for each lane. Second, the amount of dynein initially present in axonemes was subtracted from the amount pelleting after addition of extract. And third, nonspecifically sedimenting dynein was determined from recombinations of extract with *pf*28 as described in Results. Nonspecific pelleting dynein was substracted to obtain the amount of dynein in recombination pellets that had actually bound to axonemes.

We initially tried recombinations with *pf*30 and observed that almost no inner arms bound including I1. Because I1 did bind to *pf*30*pf*28 we concluded that the outer arms, present in *pf*30 block access of the inner arms to inner arm positions. This observation may be relevant for future experiments invoking immunolocalization.

Electron Microscopy

For thin section electron microscopy, specimens were fixed with 1% glutaraldehyde and 1% tannic acid in 0.1 M sodium cacodylate, post-fixed in osmium tetroxide, dehydrated in a graded series of ethanol, and embedded in Medcast-Araldite resin (Ted Pella, Inc., Irvine, CA). Uniform silver-grey sections were mounted on Formvar-coated, carbon-stabilized copper grids, stained with uranyl acetate and Reynolds lead citrate, and examined

at 80 kV in an electron microscope (model 100-CX; JEOL USA, Electron Optics Div., Peabody, MA). Transverse and longitudinal sections of reconstituted *pf*30*pf*28 axonemes were selected and analyzed as described previously (Piperno et al., 1990). Analysis of extracted and reconstituted extracted axonemes was complicated since after two extractions axonemes do not usually retain their inherent nine plus two arrangement. The doublet microtubules tend to dissociate from one another forming sheets or small groups of doublets rather than the typical circular arrangement. Therefore, in a given section thickness, orientation of the observed structures may not be obvious. For the purpose of analysis, images were selected based on our ability to recognize only pairs of spokes derived from the doublet and bound inner arms in question. All results represent data from at least three different experiments.

Sliding Disintegration

All sliding disintegration experiments were performed as described in Okagaki and Kamiya (1986) and were carried out in Buffer A minus protease inhibitors (Buffer A-PI). Flagella were sonicated with a Kontes cell disrupter (Kontes, Vineland, NJ) at a power of six yielding transversely fractured flagellar bits one-half to one-third the original length. The flagellar bits were then demembranated by adding NP-40 to a final concentration of 0.5% (wt/vol). The axoneme fragments were perfused into a 6-7 μl perfusion chamber constructed from a glass slide and cover slip (18 mm^2) separated by two strips of double-stick tape. Nonsticking axonemes were washed away with Buffer A-PI made 1 mM in ATP. Sliding disintegration was induced by perfusing the axonemes with Buffer A-PI with 1 mM ATP and 1–2 μg/ml Nagarse (Type XXVII Protease; Sigma Chemical Co., St. Louis, MO) and was recorded on video tape using a SIT camera and darkfield microscopy as described (Sale and Fox, 1988). Performing sliding disintegration with extracted axonemes did not require earlier sonication. All sliding velocities were measured manually.

General Biochemical Methods

ATP was purchased from Boehringer Mannheim Diagnostics (Houston, TX). NP-40 was purchased from Calbiochem-Behring Corp. (San Diego, CA). Other materials were reagent grade and purchased from Sigma Chemical Co. Deionized water was used throughout.

Protein measurements for all experiments were made by using the Bradford reagent (Bradford, 1976) supplied by Bio-Rad Laboratories (Richmond, CA).

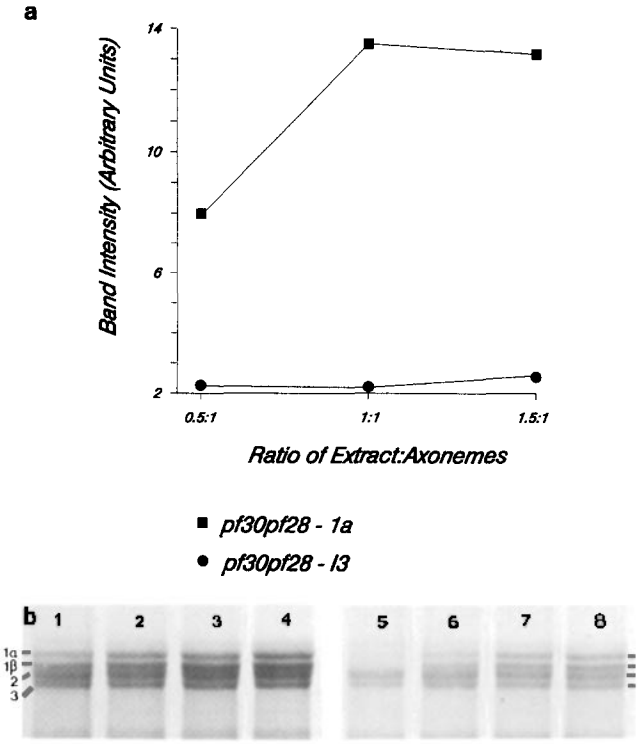

Figure 2. Densitometry (*a*) and corresponding Coomassie blue-stained gel electrophoretogram (*b*) of recombinations of extract with *pf*28 (lanes *1–4*) and *pf*30*pf*28 (lanes *5–6*) axonemes. For *b*, lanes *1–4* and lanes *5–6* represent recombination ratios of extract to axonemes at 0:1, 0.5:1.0, 1:1, and 1.5:1.0, respectively. In recombinations with *pf*30*pf*28, 1α and 1β bind appreciably and saturate at the predicted ratios for specific binding whereas I2 and I3 do not bind in significant amounts. See Materials and Methods for description of calculating band intensity values.

Results

Inner Arm Dynein I1 Rebinds to pf30pf28 Axonemes at the Predicted Stoichiometry

To assess specificity of inner arm subform binding we adopted two complimentary approaches. First, we tested whether only the correct inner dynein arm subform in a mixture of all subforms was able to bind to axonemes where only one subform position was available. Second, we tested the ability of each inner arm subform to recognize and bind to only the correct location on the axonemal doublet microtubules in which all dynein positions were vacant.

For the first approach we adopted *pf*30*pf*28 as our model since this mutant is missing the outer arms and a single inner arm subform, I1. The high salt dynein extract from *pf*28 axonemes, which contains all inner arm subforms but no outer arms, was first dialyzed in Buffer A and then mixed with *pf*30*pf*28 axonemes at various ratios based on the original volumes. For control measurements of nonspecific binding, the salt extract was also mixed with unextracted *pf*28 axonemes in which no inner arm positions are available. The resulting pellets and supernatants (supernatants not shown) were run on polyacrylamide gels and the heavy chain composition were analyzed (Fig. 2). According to Smith and Sale (1991; Methods section) we resolve only four of the six inner arm heavy chains with these electrophoretic conditions. Heavy chains 2 and 2′ comigrate and heavy chains 3 and 3′ generally comigrate; these bands are labeled 2 and 3, respectively, on all figures. Since each pair corresponds to a single inner dynein arm subtype, the interpretation of the results was unaffected.

In the control, Fig. 2 *b*, lanes *1–4*, the intensity of the dynein heavy chains increased only slightly with increasing amounts of extract added to *pf*28 axonemes. Densitometry (not shown) indicated that for each heavy chain the increase was linear with increasing dynein addition. However, electron microscopy (not shown) of the pellet at the highest ratio of extract to axoneme revealed no inner arms bound to outer arm positions or other obvious sites. Centrifugation of the extract alone did not result in dynein pelleting, indicating that the dynein was probably not aggregating into large sedimenting particles. Therefore, we felt that the dynein pelleting with *pf*28 axonemes did not represent specific binding of the inner arms but rather nonspecific co-sedimentation. Subsequently, these intensities were subtracted from measurements of *pf*30*pf*28 axoneme/dynein recombinations.

Despite the presence of all inner dynein arm subforms in the extract, the heavy chains of I1, 1α and 1β predominantly bound to *pf*30*pf*38 axonemes (Fig. 2 *b*, lanes *5–8*). Bands 1α and 3 were chosen for densitometric analysis based on convenience since they are the most easily identified. After

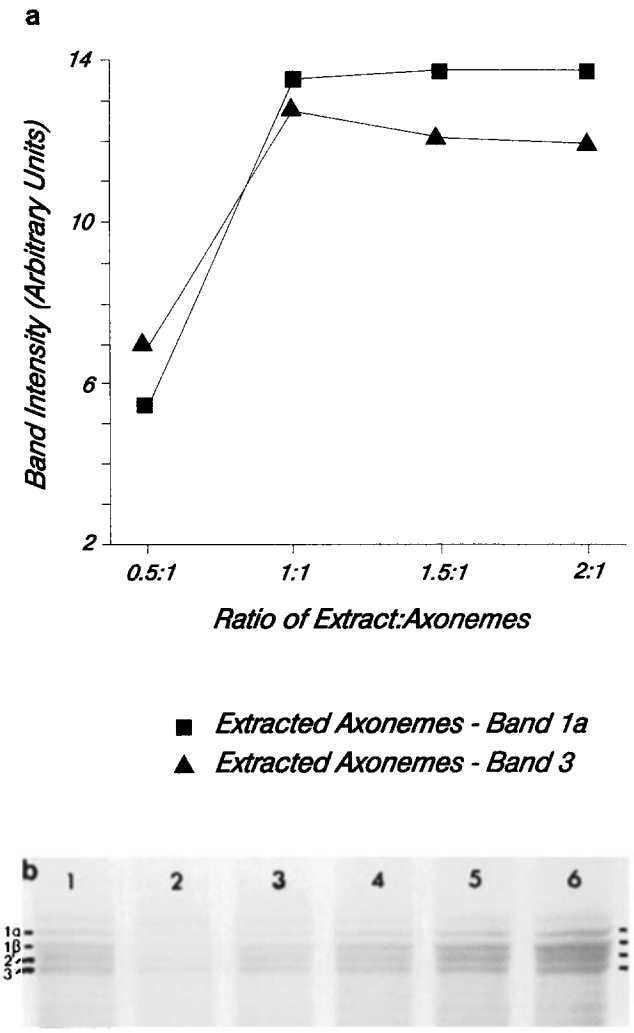

Figure 3. Densitometry (*a*) and corresponding Coomassie blue–stained gel electrophoretogram (*b*) of recombinations of extract with extracted axonemes from *pf*28. For *b*, lane *1* shows the unextracted axonemes and lanes *2–5* show recombination ratios of extract to extracted axonemes at 0:1, 0.5:1.0, 1:1, 1.5:1.0, and 2:1, respectively. All heavy chains rebind to the extracted axonemes and saturate at the predicted ratios for specific binding.

baseline subtraction, densitometry of band 3 and band 1α indicated the I3 did not bind appreciably to the axonemes whereas I1 bound in significant amounts and saturated at the predicted ratio for specific binding (Fig. 2 *a*). Several possibilities exist for the small amount of I3 pelleting with *pf*30*pf*28 axonemes. First, small amounts of dynein heavy chain in the extract are proteolyzed during the extraction procedure. Fragments of I1 may bind to axonemes but migrate on polyacrylamide gels at the I3 position. Second, during axoneme isolation, some I3 positions may become vacant so that the amount pelleting represents I3 binding to I3 positions. Or third, a small amount of I3 may bind to I1 positions; based on relative intensities, I3 would at most bind to ~10–15% of available I1 positions. Nonetheless these results indicated that extracted inner arm dynein components did not bind to open outer arm positions and that I1 specifically bound to the vacant I1 positions. This result was also quantitatively reflected in analysis of the resulting supernatants (not shown). This hypothesis was confirmed by electron microscopy shown below.

As a further test of binding specificity to the I1 position, we performed a similar reconstitution experiment using isolated inner arm components from sucrose gradient fractions. One hypothesis was that in whole extracts, I1 simply outcompetes I2 and I3 for the I1 position on the A-microtubule. We tested this hypothesis by recombining *pf*30*pf*28 axonemes with either the 21S–I1-containing or the 11S–I2,I3-containing fractions from sucrose gradients. The results were the same: the 21S, I1 fraction bound, whereas the I2 and I3 components from the 11S fraction did not, despite the availability of I1 positions and absence of competing I1 (data not shown). This experiment did not eliminate the possibility that the extracted I2 and I3 components were damaged and unable to rebind to microtubules in the pelleting assay. However, as demonstrated in the next section, I2 and I3 did rebind to doublet microtubules in the predicted amounts when I2 and I3 positions were available.

I2 and I3 Rebind to Extracted Axonemes

For the second approach to reconstitution we used *pf*28 axonemes which had been depleted of dynein. This approach offered the opportunity to examine specificity of binding of isolated dynein subforms when most or all of the dynein arm positions were vacant. The control (Fig. 3 *b*, lane *2*) indicated that not all of the inner arms were extracted to the same degree. Notably, band 3 appeared to resist extraction more than other heavy chains. The dynein extract was added to unextracted and extracted axonemes in various ratios, and gel electrophoresis was performed on the resulting pellets. As described above, a baseline was derived from recombinations with unextracted axonemes and adopted as a baseline that was subtracted from recombinations with extracted axonemes. Comparing band 3 and band 1α to control axonemes revealed that for extracted axonemes, both I1 and I3 inner arm subforms bound and saturated at a 1:1 ratio of extract to axonemes (Fig. 3 *a*). Again, analysis of resulting supernatants also revealed saturation. These results are consistent with a model in which each inner arm subform recognizes and binds only to its appropriate position on axonemal doublets. Binding of I2 and I3 to axonemes was surprising in light of our previous results demonstrating that neither bound to purified microtubules (Smith and Sale, 1991). Thus the axoneme may contain specialized tubulin isoforms or nontubulin proteins required for I2 and I3 binding (see Discussion).

To further examine the question of specificity of I2 and I3 binding and to overcome difficulties in estimating the predicted stoichiometry of isolated proteins relative to vacant dynein positions, we used the salt extract from *pf*30*pf*28 and the resulting dynein-depleted axonemes for recombinations. The dialyzed extracts contained only components of I2 and I3 and could be mixed in well-defined ratios with the axonemes from which they were derived. Fig. 4 *a* shows the resulting densitometry of inner arm heavy chain bands in the resulting pellets. (In this experiment, the amount of dynein remaining after extraction was not subtracted from recombinations with extract.) Notably, for both I2 and I3, binding saturates at the predicted ratio for specific binding. Analysis of supernatants also revealed saturation (not shown). Thus, these results suggest that I2 and I3 rebind to their original

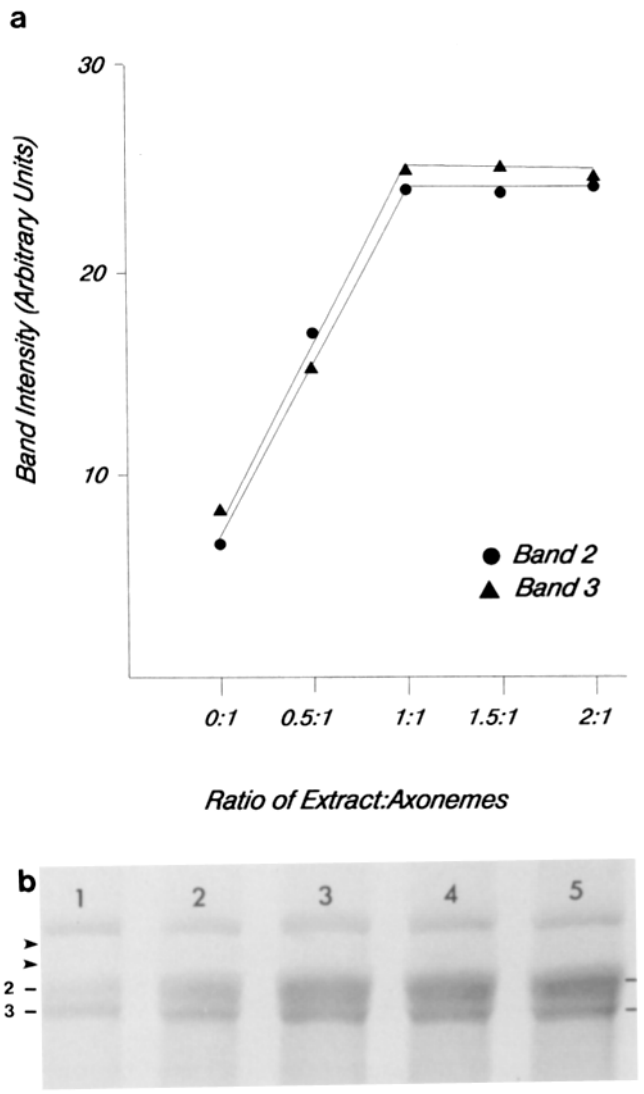

Figure 4. Densitometry (*a*) and corresponding Coomassie blue-stained gel electrophoretogram (*b*) of recombinations of extract with extracted axonemes from *pf*30*pf*28. For *b*, lanes *1–5* represent recombination ratios of extract to extracted axonemes of 0:1, 0.5:1.0, 1:1, 1.5:1.0, and 2:1, respectively. I2 and I3 bound to the extracted axonemes and saturated at the predicted ratios for specific binding. In this experiment, the control 0:1 recombination was not subtracted from subsequent recombinations but was included to compare the amount of unextracted dynein to the amount that binds. Arrowheads indicate approximate position of bands 1α and 1β in *pf*28 axonemes. The heavy protein band at the top of the gel is not a dynein component based upon genetic and biochemical analysis (Piperno et al., 1990).

positions and do not bind to vacant outer arm sites or vacant I1 positions on extracted axonemes. This conclusion is further supported by structural studies described below.

Structural Evidence for Binding Specificity

Thin section electron microscopy was performed on the pellets from axonemes mixed with excess dynein extract. Fig. 5 *a* shows *pf*30*pf*28 axonemes under ordinary buffer conditions. As described previously (Piperno et al., 1990), gaps in the inner arm I1 position are present just proximal to spoke 1 and repeat every 96 nm (Fig. 5 *a*, *arrowheads*). Upon addition of saturating amounts of either whole extracts from *pf*28 axonemes (Fig. 5 *b*) or the 21S, I1-containing fraction from sucrose gradients (not shown), gaps in the row of inner dynein arms are no longer seen (Fig. 5 *b*, *arrow*), and based upon transverse and longitudinal structural analysis, no inner arms are bound in the outer arm positions. In fact, the reconstituted axonemes are indistinguishable from *pf*28 axonemes (Fig. 5 *c*) indicating that I1 bound only to its original position, consistent with the biochemical analysis described above.

Structural studies with extracted axonemes were more challenging. First, we showed in gels above that heavy chain material is not completely removed from extracted axonemes. For ultrastructural studies, we twice extracted the axonemes but small amounts of I3 still remained and could be seen occasionally in electron micrographs. Second, to assess specificity of dynein subform binding, polarity for the extracted axonemes had to be determined. Originally, we used the tilt of the outer dynein arms but this was obviously impossible in the case of outer dynein armless mutant and extracted axonemes. Previously, we noted the appearance of a small electron dense structure under spoke 1 in *pf*23 and *pf*30 axonemes, which are both missing I1 (see Fig. 8; Piperno et al., 1990). In high-salt, extracted axonemes this structure remains and can serve as a marker identifying spoke 1 and consequently permit determination of polarity. In those occasional axonemes which were incompletely extracted, I3 could be distinguished from the electron-dense structure under spoke 1 based on relative size, since I3 is larger.

Extracted axonemes were recombined with excess of either the 21S-I1-containing fraction or the 11S-I2,I3-containing fraction. Fig. 6 *a* shows a longitudinal image of a control-extracted doublet with the proximal end to the left based upon the structure located under and just proximal to spoke 1 (*arrowheads*). When the extracted axonemes were recombined with the 21S fraction (Fig. 6 *b*) the density under the proximal to spoke 1 appeared to increase in size indicating that I1 rebound in the correct position. To confirm this observation, length measurements were made of the electron-dense material in the I1 position for individual spoke pair groups. The electron-dense material just proximal to spoke 1 in extracted axonemes alone measured 23 $\pm$ 4 nm (n = 69), whereas the material in the same position after adding the 21S fraction averaged 57 $\pm$ 7.7 nm (n = 57). If we assume that this material represents both I1 and the inextractable material and subtract the amount contributed by the inextractable material from the total amount, we estimate that 34 nm is contributed by I1 alone (c.f., Piperno et al., 1990). This measurement is remarkably close to one-third the total 96 nm repeat period for the inner arms.

Occasionally, I1 binds directly underneath and just distal to spoke 1 leaving a space between the inextractable material and the dynein arm (Fig. 6 *b*, *asterisks*). In 18 out of 57 spoke pair groups analyzed (or 32% of the time) this arrangement occurred. Earlier analysis of isolated I1 revealed two-headed particles with particularly large stem domains (Smith and Sale, 1991). Possibly, I1 that has bound to the correct A-microtubule site is somewhat flexible, and the bulk of its mass occasionally flops to the more distal side of spoke 1. This possibility is also supported by our observations that at no time was I1 seen to bind under spoke 2.

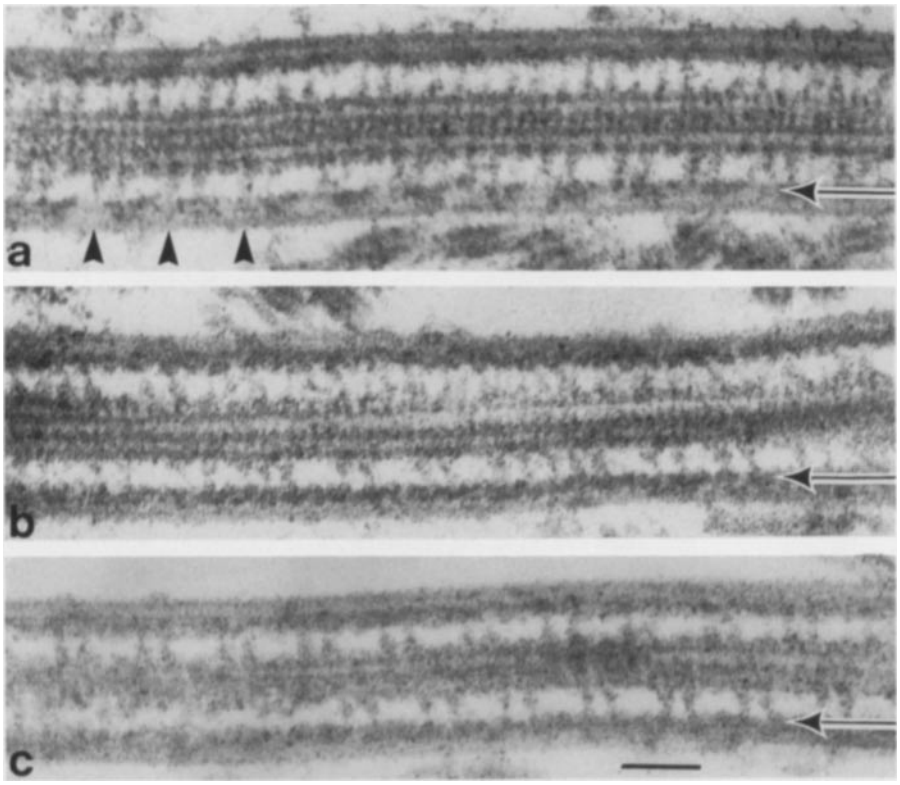

Figure 5. Longitudinal sections of *pf*30-*pf*28 (*a*), reconstituted *pf*30*pf*28 (*b*), and *pf*28 axonemes (*c*). Arrows indicate the row of inner dynein arms. Arrowheads (*a*) indicate gaps in the row of inner arms for *pf*30*pf*28 axonemes. Bar, 100 nm.

The most striking feature of these recombinations is that for all experiments and all axonemes examined, binding was periodic with large regularly repeating gaps between the bound material. If I1 were capable of binding to other locations then predictably no gaps, or perhaps aperiodic gaps, in the row of inner arms would be observed under the saturating conditions used. Therefore, this periodicity alone is strong evidence that I1 recognizes the correct location on the axoneme.

In recombinations of extracted axonemes with the 11S fraction containing a mixture of I2 and I3, binding of inner arms was observed both proximal and distal to spoke 2, and was distinct from the inextractable material under spoke 1 (Fig. 6 *c*). The average length of the I2,I3 material was 50.9 ± 4.8 nm (n = 23). This measurement compares well with that in *pf*30*pf*28 axonemes in which the average length of the remaining inner arms, I2 and I3, is 57 ± 6 nm, indicating that both subforms are rebinding to the extracted axonemes. Identical results were obtained in recombinations with *pf*30*pf*28 extracts containing only I2 and I3 that were recombined with extracted axonemes (not shown). In either case the binding was extremely periodic with regular intervening gaps. Therefore, in support of results described above, I2 and I3 also appear to recognize the correct position on the extracted axonemes.

Addition of Inner Arm Subforms Restores Microtubule Sliding Velocity

To assess functional restoration of reconstituted axonemes we used the sliding disintegration assay adapted for *Chlamydomonas* flagellar axonemes (Okagaki and Kamiya, 1986). Microtubule sliding disintegration results were reliable and afforded a direct comparison of microtubule sliding velocities between axonemes from mutant and wild-type cells as well as reconstituted axonemes. These results are both summarized in Fig. 7.

For comparison of microtubule sliding velocities for *pf*30*pf*28 and *pf*28 axonemes, flagella were sonicated and demembranated as described in Materials and Methods. Under conditions of 1 mM ATP the *pf*30*pf*28 axonemal doublets slid apart at 0.72 μm/s (±0.36 μm/s, n = 33), whereas *pf*28 doublets slid at 1.33 μm/s (±0.47 μm/s, n = 43), or almost twice the velocity of *pf*30*pf*28 (significantly different $P < 0.001$). After the addition of the I1 containing 21S fraction from sucrose gradients to both types of axonemes, *pf*28 sliding velocities remained the same (1.48 μm/s ± 0.47, n = 30). In contrast, *pf*30*pf*28 reconstituted with I1 microtubule sliding velocities increased to that of *pf*28 (1.51 μm/s ± 0.68, n = 20) (Fig. 7). Therefore, not only did isolated I1 recognize and bind to its correct position, but it was also functionally active.

The sliding disintegration assay was also used to investigate whether isolated dynein subforms could restore doublet sliding in axonemes depleted of dynein by salt extraction. For these experiments, flagella were not sonicated to prevent dissociation of the doublets after demembranation and salt extraction. As a control, flagella were simply demembranated and applied to the sliding disintegration assay without sonication. Although the number of axonemes sliding in a given field is slightly lower than when using axonemal fragments, microtubules from most of the axonemes do slide apart and at the same velocity as when sonicated.

After control measurements, nonsonicated isolated axonemes were extracted in high-salt as described in Materials and Methods. For both *pf*28 and *pf*30*pf*28, extracted axonemes under identical experimental conditions were never

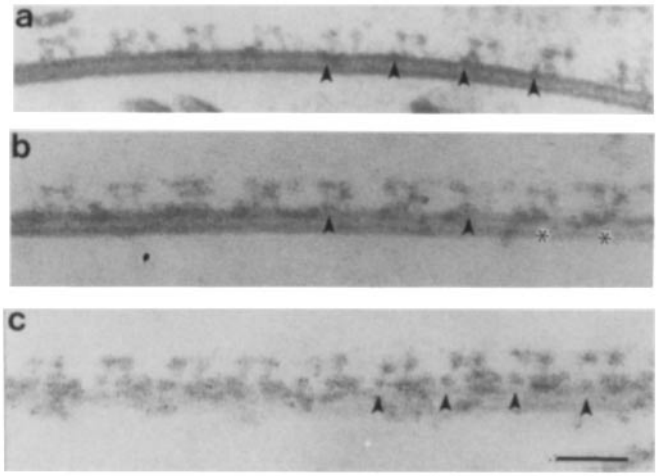

Figure 6. Longitudinal sections of a control extracted doublet (*a*), an extracted doublet recombined with the 21S–I1-containing fraction (*b*), and an extracted doublet recombined with the 11S–I2,I3-containing fraction. Arrowheads indicate the inextractable structure located under spoke 1 that was used as a polarity marker. Asterisks indicate areas where I1 is located distal to spoke 1. Bar, 100 nm.

seen to undergo sliding disintegration. In contrast, extracted *pf*30*pf*28 axonemes recombined with the dynein extract derived from *pf*30*pf*28, slid at the same velocity as before extraction (0.68 μm/s, ± 0.12, n = 12; Fig. 7). Similarly, extracted *pf*28 axonemes when recombined with the dynein extract derived from *pf*28 axonemes also slid at the same velocity as before extraction (1.3 μm/s, ± 0.47, n = 20; Fig. 7). These results provide evidence that all of the reconstituted inner dynein arm are functionally active.

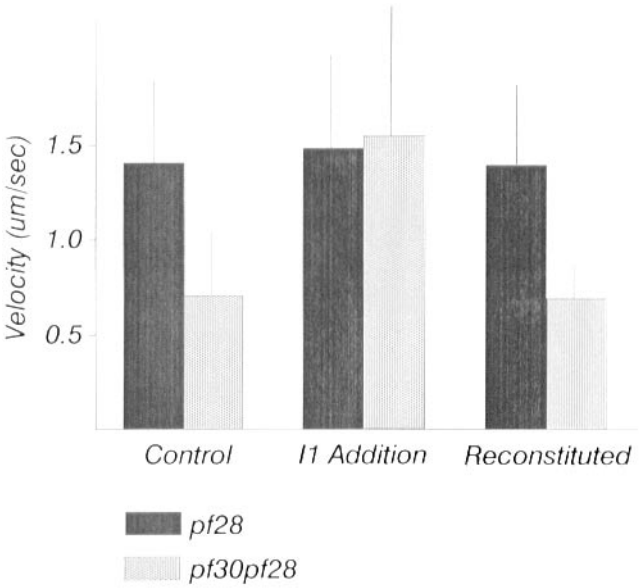

Figure 7. Histogram of protease induced microtubule doublet sliding velocities in 1 mM ATP. The reconstituted axonemes represent extracted *pf*28 and *pf*30*pf*28 axonemes recombined with their respective extracts.

Discussion

Using a combination of biochemical, structural, and functional techniques, we provide data indicating that isolated inner dynein arm subtypes rebind to specific sites on axonemal doublet microtubules. The simplest model derived from these observations is that the site of assembly of each inner arm is dictated by the position of regularly repeating receptor or adaptor molecules on the A-microtubule of each doublet. Candidate molecules could include specially adapted and highly localized tubulin isoforms and/or other nontubulin proteins which resist extraction with high-salt buffers. The results also indicate that structural domains responsible for axonemal microtubule binding differ for each inner arm dynein subform.

Several results indicate that isolated inner arm dyneins rebind selectively and specifically to doublet microtubules. Based on densitometry of Coomassie blue-stained gels, the binding of subform I1 to either *pf*30*pf*28 or extracted axonemes saturated at the correct stiochiometry indicative of specific binding to the I1 position on axonemes. This was confirmed by electron microscopy where I1 in either whole extracts or the 21S sucrose gradient fraction bound only to the I1 position with the predicted periodicity in both *pf*30*pf*28 axonemes and extracted axonemes. Evidently, the defect in *pf*30 is not in the microtubule or dynein receptor function, but may be in a component required for proper assembly and/or transport.

Densitometry of heavy chains representing I2 and I3 indicated that these subforms, in either extracts or the 11S sucrose gradient fraction, did not bind appreciably to *pf*30*pf*28 axonemes. Yet, both bound to extracted axonemes of *pf*30-*pf*28 and *pf*28 and saturated at ratios of extract to axonemes indicative of site-specific recognition and attachment. Electron microscopy of these recombinations with either extracted *pf*28 or *pf*30*pf*28 axonemes revealed that I2 and I3 rebound to the correct positions in a periodic fashion. Warner et al. (1985) reported a similar periodic rebinding in recombinations of extracted 13S dynein with the extracted ciliary axonemes of *Tetrahymena*. Although the exact source of the 13S dynein was not clear, this dynein rebound to the inner dynein arm positions with a periodicity corresponding to that of the repeating spoke groups. Together, our results indicate that each inner dynein arm only recognizes a specific position along the A-microtubule of the doublet. However, we can not rule out the possibility that a structural feature of the B-microtubule of the adjacent doublet also contributes to specificity of rebinding although this seems unlikely since dyneins appear to bind specifically to isolated doublets (Fig. 6).

In earlier studies we discovered that isolated I1 binds to single microtubules, assembled in vitro from purified tubulin, in irregular, random positions (Smith and Sale, 1991). Thus, it is curious why we did not visualize I1 binding to random positions on axonemal microtubules. Possibly, we were unable to recognize nonspecific structural binding, or I1 only binds to its designated position. The earlier observation of random binding of I1 to microtubules is also consistent with the hypothesis that doublet microtubules contain specialized adaptor molecules that designate the precise location of each inner arm subform since isolated inner arms will not bind to purified microtubules correctly. Further, the mechanism by which inner arms bind to A-microtubules is apparently very

different from the mechanism used by the outer arms. In contrast to the inner arms, the outer arms isolated from *Chlamydomonas* flagella bind in the same manner to both purified microtubules and doublet microtubules suggesting that correct assembly of outer arms does not require other nontubulin proteins (c.f., Haimo et al., 1979; Haimo and Fenton, 1984). However, other evidence indicates that the outer arms will only rebind to specific positions around the circumference of the A-microtubule (Gibbons and Gibbons, 1979; Sakakibara and Kamiya, 1989), indicating some form of recognition also occurs for the outer arms.

Unfortunately, we have so far been unable to separate the components of I2 and I3 from each other to confirm that each is binding to its respective position. We also do not know whether each type of homodimer is binding to the proper proximal and distal regions as in vivo. One approach to investigating this problem would be to use *pf*23*pf*28 axonemes for recombination since they are missing both I1 and I2 but contain I3. However, this experiment has not succeeded due to the extremely short flagella in *pf*23*pf*28. Another approach would be to use antibodies specific for the individual subforms to monitor the composition of structures bound to precise locations along microtubules. However, useful antibodies are not yet available.

Our results demonstrated that the reconstituted inner arm dyneins are functionally active. For functional studies we used a quantitative microtubule sliding assay in which we directly compared microtubule sliding velocity in control and reconstituted axonemes. Comparing the microtubule sliding velocities of *pf*30*pf*28 axonemes with that of *pf*28, the *pf*30*pf*28 axonemes slid at half the velocity of *pf*28 axonemes. After the addition of I1 from either whole extracts or from the 21S fraction of sucrose gradients, the reconstituted *pf*30*pf*28 axonemes slid at the same velocity as *pf*28 axonemes suggesting complete restoration of functional arms. These results were unexpected given our previous findings using isolated I1 in an in vitro microtubule gliding assay (Smith and Sale, 1991). In this assay the isolated dynein was adsorbed to a glass slide by perfusion, and microtubules in an ATP-containing buffer were then perfused into the chamber and observed to bind to and glide across the dynein-coated surface. We found that the 21S-I1-containing gradient fraction supported very slow and often irregular microtubule gliding. We concluded that either I1 did not contribute directly to microtubule sliding velocity or that the gliding assay was not suitable for investigating its microtubule translocating properties. Given our new results the latter appears to be the case, and, thus, I1 does contribute, either directly or indirectly, to microtubule sliding velocities in axonemes.

Ideally we would like to have restored reactivated motility to *pf*30*pf*28 by adding the missing inner dynein arm I1. This experimental approach was first used by Gibbons and Gibbons (1976, 1979) and later by Sakakibara and Kamiya (1989) to demonstrate that isolated outer arm dynein can specifically rebind to vacant outer arm sites and restore normal beat frequency to reactivated axonemes. So far we have been unable to reactivate axonemes from *pf*30*pf*28 after reconstitution with I1. This might be due to technical difficulties not yet identified or due to other unidentified components in addition to I1 also missing in *pf*30*pf*28 and necessary for motility.

We also used the quantitative sliding disintegration assay to assess the functional activity of dynein extracts after recombination with extracted axonemes. Extracted axonemes alone never underwent microtubule sliding disintegration, however, reconstituted extracted axonemes regained full pre-extraction sliding velocities. Evidently, each of the solubilized inner arm dyneins remains functionally active. This result was surprising since we originally suspected that the high-salt treatment would alter the axonemes and render functional restoration impossible. Thus, extracted axonemes may be of significant use in reconstitution experiments that will enable us to identify and define components that affect not only the specificity of dynein binding but also the functional regulation of dynein in the axoneme. We are currently using this and other approaches to identify such components.

We would like to thank Dr. Harish Joshi for critically reading the manuscript.

This work was supported by National Institutes of Health Training Grant GM08367-02 and National Institutes of Health Research Grant HD 20497.

Received for publication 1 October 1991 and in revised form 20 November 1991.

References

Bradford, M. M. 1976. A rapid and sensitive method for the quantitation of microgram quantities of proteins utilizing the principal of protein dye binding. *Anal. Biochem.* 72:248–284.

Brokaw, C. J., and R. Kamiya. 1987. Bending patterns of *Chlamydomonas* flagella IV: mutants with defects in inner and outer dynein arms indicate differences in arm function. *Cell Motil. Cytoskeleton.* 8:68–75.

Gibbons, B. H., and I. R. Gibbons. 1976. Functional recombination of dynein 1 with demembranated sea urchin sperm partially extracted with KC1. *Biochem. Biophys. Res. Commun.* 73:1–6.

Gibbons, B. H., and I. R. Gibbons. 1979. Relationship between the latent adenosine triphosphatase state of dynein 1 and its ability to recombine functionally with KCL-extracted sea urchin sperm flagella. *J. Biol. Chem.* 254: 197–201.

Goodenough, U. W., and J. E. Heuser. 1982. Substructure of the outer dynein arm. *J. Cell Biol.* 95:798–815.

Goodenough, U. W., and J. E. Heuser. 1985. Substructure of inner dynein arms, radial spokes, and the central pair projection complex of cilia and flagella. *J. Cell Biol.* 100:2008–2018.

Goodenough, U. W., and J. E. Heuser. 1989. Structure of the soluble and *in situ* ciliary dyneins visualized by quick-freeze deep-etch microscopy. *In* Cell Movement. Vol. 1. F. D. Warner, P. Satir, and I. R. Gibbons, editors. Alan R. Liss, Inc., New York. 121–140.

Haimo, L. T., and R. Fenton. 1984. Microtubule crossbridging by *Chlamydomonas* dynein. *Cell Motil.* 4:371–385.

Haimo, L. T., B. R. Telzer, and J. L. Rosenbaum. 1979. Dynein binds to and crossbridges cytoplasmic microtubules. *Proc. Natl. Acad. Sci. USA.* 76:5659–5763.

Kagami, O., S. Takada, and R. Kamiya. 1990. Microtubule translocation caused by three subspecies of inner-arm dynein from *Chlamydomonas* flagella. *FEBS (Fed. Eur. Biochem. Soc.) Lett.* 264:2:179–182.

Kamiya, R., and M. Okamoto. 1985. A mutant of *Chlamydomonas reinhardtii* that lacks the flagellar outer dynein arm but can swim. *J. Cell Sci.* 74:181–191.

Kamiya, R., E. Kurimoto, and E. Muto. 1991. Two types of *Chlamydomonas* flagellar mutants missing different components of inner-arm dynein. *J. Cell Biol.* 112:441–447.

King, S. M., T. Otter, and G. B. Witman. 1986. Purification and characterization of *Chlamydomonas* flagellar dyneins. *Methods Enzymol.* 134:291–305.

Laemmli, U. K. 1970. Cleavage of structural proteins during the assembly of the head of bacteriophage T4. *Nature (Lond.).* 227:680–685.

Mitchell, D., and J. L. Rosenbaum. 1985. A motile *Chlamydomonas* flagellar mutant that lacks outer dynein arms. *J. Cell Biol.* 100:1228–1234.

Muto, E., R. Kamiya, and S. Tsukita. 1991. Double-rowed organization of inner dynein arms in *Chlamydomonas* flagella revealed by tilt series thin-section electron microscopy. *J. Cell Sci.* 99:57–66.

Okagaki, T., and R. Kamiya. 1986. Microtubule sliding in mutant *Chlamydomonas* axonemes devoid of outer or inner dynein arms. *J. Cell Biol.* 103:1895–1902.

Piperno, G., and Z. Ramanis. 1991. The proximal portion of *Chlamydomonas* flagella contains a distinct set of inner dynein arms. *J. Cell Biol.* 112:701–709.

Piperno, G., Z. Ramanis, E. F. Smith, and W. S. Sale. 1990. Three distinct inner dynein arms in *Chlamydomonas* flagella: molecular composition and location in the axoneme. *J. Cell Biol.* 110:379–389.

Sakakibara, H. and R. Kamiya. 1989. Functional recombination of outer dynein arms with outer arm-missing flagellar axonemes of a *Chlamydomonas* mutant. *J. Cell Sci.* 92:77–83.

Sale, W. S., and L. A. Fox. 1988. Isolated β-heavy chain subunit of dynein translocate microtubules *in vitro*. *J. Cell Biol.* 107:1793–1798.

Sale, W. S., U. W. Goodenough, and J. E. Heuser. 1985. The substructure of isolated and in situ outer dynein arms of sea urchin sperm flagella. *J. Cell Biol.* 101:1400–1412.

Smith, E. F., and W. S. Sale. 1991. Microtubule binding and translocation by inner dynein arm subtype I1. *Cell Motil. Cytoskeleton.* 18:258–268.

Warner, F. D., J. G. Perreault, J. H. McIlvain. 1985. Rebinding of *Tetrahymena* 13S and 21S dynein ATPases to extracted doublet microtubules. *J. Cell Sci.* 77:263–287.

Witman, G. B. 1986. Isolation of *Chlamydomonas* flagella and flagellar axonemes. *Methods Enzymol.* 134:280–290.

Witman, G. B., J. Plummer, and G. Sander. 1978. *Chlamydomonas* flagellar mutants lacking radial spokes and central tubules. *J. Cell Biol.* 76:729–747.